Inhibition of gingipains by their profragments as the mechanism protecting *Porphyromonas gingivalis* against premature activation of secreted proteases

Florian Veillard[1,#], Maryta Sztukowska[1,#], Danuta Mizgalska[2], Mirosław Ksiazek[2], John Houston[1], Barbara Potempa[1], Jan J. Enghild[3], Ida B. Thogersen[3], F. Xavier Gomis-Rüth[4], Ky-Anh Nguyen[5,6], Jan Potempa[1,2,*]

[1]Oral Health and Systemic Diseases Research Group, University of Louisville School of Dentistry, Louisville, KY 40202, USA; e-mails: florian.veillard@gmail.com; mnsztu01@louisville.edu; jahous05@lousville.edu; bapote01@louisville.edu; jspote01@louisville.edu

[2]Department of Microbiology, Faculty of Biochemistry, Biophysics and Biotechnology, Jagiellonian University, 30-387 Krakow, Poland. e-mails: dankamizgalska@gmail.com; ksiazek.miroslaw@gmail.com; jan.potempa@uj.edu.pl

[3]Center for Insoluble Protein Structures (inSPIN) and Interdisciplinary Nanoscience Center (iNANO) at the Department of Molecular Biology and Genetics, Aarhus University, Aarhus DK-8000, Denmark; e-mails: jje@mb.au.dk; ibt@mb.au.dk

[4]Proteolysis Lab, Molecular Biology Institute of Barcelona, Spanish Research Council CSIC, Barcelona Science Park, c/Baldiri Reixac 15-21, 08028 Barcelona, Catalonia (Spain); e-mail: xgrcri@ibmb.csic.es

[5]Institute of Dental Research, Westmead Centre for Oral Health and Westmead Millenium Institute, Sydney NSW 2145, Australia; e-mail: kyanhn@gmail.com

[6]Faculty of Dentistry, University of Sydney, Sydney NSW 2006, Australia.

[#]These authors contributed equally to this study and share first authorship.

*Corresponding author phone number: (+1) 502-852-1319

Abbreviations: PD, N-terminal prodomain; CD, catalytic domain; CTD, C-terminal domain

ABSTRACT

Background: Arginine-specific (RgpB and RgpA) and lysine-specific (Kgp) gingipains are secretory cysteine proteinases of *Porphyromonas gingivalis* that act as important virulence factors for the organism. They are translated as zymogens with both N- and C-terminal extensions, which are proteolytically cleaved during secretion. In this report, we describe and characterize inhibition of the gingipains by their N-terminal prodomains to maintain latency during their export through the cellular compartments.

Methods: Recombinant forms of various prodomains (PD) were analyzed for their interaction with mature gingipains. The kinetics of their inhibition of proteolytic activity along with the formation of stable inhibitory complexes with native gingipains was studied by gel filtration, native PAGE and substrate hydrolysis.

Results: PD_{RgpB} and PD_{RgpA} formed tight complexes with arginine-specific gingipains (Ki in the range from 6.2 nM to 0.85 nM). In contrast, PD_{Kgp} showed no inhibitory activity. A conserved Arg-102 residue in PD_{RgpB} and PD_{RgpA} was recognized as the P1 residue. Mutation of Arg-102 to Lys reduced inhibitory potency of PD_{RgpB} by one order of magnitude while its substitutions with Ala, Gln or Gly totally abolished the PD inhibitory activity. Covalent modification of the catalytic cysteine with tosyl-L-Lys-chloromethylketone (TLCK) or H-D-Phe-Arg-chloromethylketone did not affect formation of the stable complex.

Conclusion: Latency of arginine-specific progingipains is efficiently exerted by N-terminal prodomains thus protecting the periplasm from potentially damaging effect of prematurely activated gingipains.

General significance: Blocking progingipain activation may offer an attractive strategy to attenuate *P. gingivalis* pathogenicity.

Keywords: pathogen; periodontitis; inhibitor; proteolysis control; zymogen activation

1. Introduction

Proteolysis plays a key role in all aspects of life processes. Since peptide bond hydrolysis is irreversible, proteolytic enzymes are tightly regulated spatially and temporally at the transcriptional and post-translational levels [1]. The latter is accomplished by many mechanisms and is well characterized in eukaryotes. Perplexingly, far less is known about post-translational control of proteolysis in prokaryotes although many of them produce copious amounts of proteases. Due to the broad specificity of many secreted enzymes, bacterial extracellular proteases are often synthesized as enzymatically inactive proforms (zymogens) [2, 3]. The zymogenic status is frequently exerted by an N-terminal profragment functioning as a tethered inhibitor, which needs to be removed by proteolysis to release the active protease [4-16]. In Gram-negative bacteria, this kind of regulation is expected to protect the periplasm from proteolytic damage. This can be especially true in the case of the periodontal pathogen *Porphyromonas gingivalis*, which is armed with large quantities of cell-surface-bound and secreted forms of cysteine proteases, referred to as gingipains [17].

Gingipains, which are products of three different genes, are essential for *P. gingivalis* pathogenicity. Two gingipains (RgpA and RgpB) are specific for Arg at the carbonyl side of the peptide bonds and the third (Kgp) cleaves after Lys residues [18]. Gingipains are responsible for nutrient generation, colonization of the periodontal tissue, dissemination, and evasion of host innate and acquired immunity [19]. The latter is accomplished predominantly by specific, limited proteolysis of key components of complement, coagulation cascade, kinin-generation pathway, and protease activated receptors, just to name few. Further, gingipains are involved in the processing of many self-proteins such as the assembly of surface fimbriae, an important virulence factor of *P. gingivalis* [20]. However, as gingipains are highly active and present in high concentrations, they can also indiscriminately degrade many other cellular proteins within *P. gingivalis* – this clearly presents a danger to the organism.

All three gingipains have typical signal peptides and translocate through the inner membrane via the Sec system. However, the mechanism of their transport across the outer membrane is still poorly understood. In strains with inactivated outer membrane translocon (referred to as PorSS), progingipains are found in the periplasm as inactive zymogens [21]. These zymogens are composed of an N-terminal prodomain (PD) of 204-209 residues, a catalytic domain (CD) of 435 (RgpB), 459 (RgpA and 508 (Kgp) residues and a conserved C-terminal domain (CTD, *circa* 70 residues), which is also present in secreted proteins from many

other periodontal pathogens [22]. The RgpA and RgpB catalytic domains are basically identical. In proRgpB, however, the CD is followed directly by the CTD, while in proRgpA and proKgp, a large hemagglutinin/adhesin domain is present between the CD and the CTD [23]. During the secretion process, both the N-terminal prodomain and the CTD are cleaved off [24]. In the majority of *P. gingivalis* strains, gingipains are retained on the cell surface. RgpB is associated with the outer membrane in the form of a heavily glycosylated protein (membrane-type RgpB; mt-RgpB) while RgpA and Kgp are assembled together into non-covalent multi-domain complexes on the bacterial surface [25]. The exception is strain HG66, which secretes soluble gingipains into growth media as a non-glycosylated form of RgpB, and separate RgpA (HRgpA) and Kgp enzymes, the latter two being complexes of the catalytic and hemagglutinin/adhesin domains [26].

Although the cellular location of progingipain processing (prior-, during- or after translocation through the outer membrane) remains to be elucidated, accumulation of enzymatically inactive progingipains in the periplasm of PorSS-deficient strains strongly suggests that progingipains are transiently present in the periplasm during the secretion process [21, 27-31]. We hypothesized that the zymogenic status of progingipains is maintained by N- or C-terminal prodomains either through direct steric blocking of the substrate-binding site, by interfering with the catalytic residues or by preventing complete folding of the catalytic domain. Here, to test the mechanism of progingipains latency, we have expressed N-terminal prodomains and analyzed their interaction with mature gingipains.

2. Material and Methods

2.1. Reagents

Bacterial growth media were sourced from Difco Laboratories (Detroit, MD, USA). Synthetic protease substrates: Nα-benzoyl-L-Arg-*p*-nitroanilide (BAPNA), acetyl-L-Lys-*p*-nitroanilide (Ac-Lys-pNA) and protease inhibitors: N-carbobenzyloxy-Phe-Phe-Arg-chloromethylketone (Z-FFR-CMK) and H-D-Tyr-Pro-Arg-chloromethylketone (YPR-FMK) were from Bachem (Torrance, CA, USA). Azocoll^{R} general protease substrate was purchased from EMD Chemicals (Philadelphia, PA) and all other substrates, protease inhibitors and general chemicals including, N-carbobenzyloxy-L-Arg-7-amino-4-methylcoumarin (Ac-Arg-AMC), H-L-Arg-7-amino-4-methylcoumarin (H-Arg-AMC), N-carbobenzyloxy-Phe-Arg-7-amino-4-methylcoumarin (Z-FR-AMC), N-carbobenzyloxy-Gly-Pro-Arg-7-amino-4-methylcoumarin (Z-GPR-AMC), N-

carbobenzyloxy-Ala-Gly-Pro-Arg-7-amino-4-methylcoumarin (Z-AGPR-AMC), tosyl-L-Lys-chloromethylketone (TLCK), and H-D-Phe-Arg-fluoromethylketone (FR-FMK), were from Sigma (St. Louis, MI, USA).

2.2. Gingipains purification

High molecular weight gingipain R (HRgpA), low molecular weight gingipain R (RgpB), and gingipain K (Kgp) were purified from cell-free medium of *P. gingivalis* HG66 by acetone precipitation, size-exclusion chromatography using Sephadex G-150, and affinity chromatography on Lysine-Sepharose as described previously [32, 33] Glycosylated, membrane-type RgpB was partially purified from the outer membrane fraction of *P. gingivalis* W83 cultured into the early stationary phase of growth [34]. All gingipains were active-site titrated to determine the active fraction [35].

2.3. Cloning, expression and purification of recombinant PDs

The pro-domains (PDs) of gingipains RgpA (Q^{24}-R^{227}), RgpB (Q^{25}-R^{229}) and Kgp (Q^{20}-R^{228}) were cloned into the pGEX-6P-1 expression vector using *Bam*HI/*Xho*I sites and the following PCR primers (restriction sites are underlined):

PD-RgpA_F: 5'-ATAGGATCCCAGCAGACAGAGTTGGG-3'
PD-RgpA_R: 5'-TTCCTCGAGTTAACGCCCTGGCTCGTACTT-3'
PD-RgpB_F: 5'-ATAGGATCCCAGCCGGCAGAGCGCGGT-3'
PD-RgpB_R: 5'-TTCCTCGAGTTAGCGCGTAGCTTCATAATTCATG-3'
PD-Kgp_F: 5'-ATAGGATCCCAAAGCGCCAAGATTAAGCTTG-3'
PD-Kgp_R: 5'-TTCCTCGAGTTAATTGAAGAGCTGTTTATAAGC-3'

The resulting recombinant product includes an N-terminal glutathione-S-transferase (GST) tag, a PreScission protease cleavage followed by the individual PD protein.
The resultant recombinant plasmids (pGEX-6P1_PD-RgpA, pGEX-6P1_PD-RgpB, and pGEX-6P1_PD-Kgp) were confirmed with DNA sequencing and transformed into *E. coli* BL21(DE3) expression host. Transformed *E. coli* hosts were grown in LB media at 37 °C, cooled to 24 °C and expression of recombinant proteins were induced by the addition of 0.1 mM isopropyl-1-thio-β-D-galactopyranoside (IPTG) at OD_{600} 0.8. After overnight cultivation, cells were harvested by centrifugation at 6,000 × g for 20 min and resuspended in PBS supplemented with lysozyme and subsequently lysed by sonication (3 cycles of 10 × 3 s pulses at 17 W). The

lysate was clarified by ultracentrifugation at 150,000 × g for 1 hour before being passed through a pre-equilibrated glutathione-Sepharose™ High Performance column (GE Healthcare, Pittsburgh, PA, USA) at room temperature. Recombinant GST-PDs were eluted using 50 mM Tris-HCl, pH 8.0, supplemented with 10 mM reduced glutathione. After overnight dialysis against 4 L of PBS, samples were incubated for 24 hours at 4 °C with the PreScission™ Protease (GE Healthcare) and subjected again to chromatography on glutathione-Sepharose™ to remove GST and uncleaved GST-PD fusion proteins. The flow-through was concentrated by ultrafiltration using a 10 kDa cut-off membrane and dialyzed against PBS. Protein concentration was determined by BCA Assay (Sigma) and purity of recombinant protein was verified by SDS-PAGE electrophoresis (NuPAGE® 4-12% Bis-Tris Gel, Invitrogen) stained with SimplyBlue™ SafeStain (Invitrogen).

The wild-type plasmid construct of PD-RgpB was used to produce Arg66Lys (R66K), Arg66Ala (R66A), Arg102Lys (R102K), Arg102Ala (R102A), Arg102Glu (R102E) and Arg102Gln (R102Q), and Arg159Lys (R159K) mutations using the QuikChange Site-Directed Mutagenesis Kit (Stratagene, La Jolla, CA, USA) following the manufacturer's instructions. The mutated constructs were verified by DNA sequencing.

2.4. CD spectroscopy

CD spectra of PDs at 0.3 mg/ml in 20 mM sodium phosphate buffer, pH 7.4, were obtained using a Jasco J-710 spectropolarimeter with 1 mm cell pathlength. Data acquisitions were made at 0.2 nm intervals with a dwell time of 1 s between 200 and 260 nm, at 20 °C and averaged from 4 repeated scans. Secondary-structure content was assessed from CD measurements by computational analysis based on Kohonen's self-organizing maps: SOMCD [36] and compared to the predicted secondary-structure content estimated by Jpred 3 [37].

2.5. Inhibition assay

Gingipains (10 nM) were pre-activated in activity assay buffer (200 mM Tris-HCl, 5 mM $CaCl_2$, 150 mM NaCl, and 0.02% NaN_3, pH 7.6, supplemented with 10 mM L-cysteine) for 10 mins at 37 °C before the addition of a range of recombinant PD concentrations (0.1 nM to 10 μM) in a total volume of 200 μl in 96-well plates. After 15 min, the residual activities against 0.5 mM chromogenic substrates L-BAPNA (for RgpB and HRgpA) or Ac-Lys-pNA (for Kgp) were recorded at 420 nm using a SpectraMax M5 spectrofluorimeter plate-reader. Effect of PDs on

aminopeptidase activity of RgpB and HRgpA was determined under the same condition using the fluorogenic substrate H-Arg-AMC (λ_{ex} = 380 nm; λ_{em} = 460 nm) [38]. Similarly, inhibition of proteolytic activity in 10 nM gingipains by PDs was determined using 100 μl of 15 mg/ml suspension of Azocoll substrate under the same condition as described above. After 2 hours at 37 °C, the reaction was stopped by addition of 100 μl of 3 M Glycine, pH 3.0 and undigested Azocoll fibers were removed by centrifugation (5 min at 10,000 × g). The absorbance at 520 nm of the clarified supernatant (200 μl) was measured in a 96-well plate using a SpectraMax M5 spectrofluorimeter plate-reader.

2.6. Determination of the inhibition mode and kinetic measurement

RgpB and HRgpA (1 nM) were incubated at 37 °C in assay buffer supplemented with 10 mM L-cysteine in the presence of increasing concentrations of PD (0 to 10 nM) in a 96-well plate. After 15 min, the fluorogenic substrate Z-Arg-AMC was added at several concentrations (0 to 30 μM) and the residual activities were recorded (λ_{exc} = 380 nm; λ_{em} = 460 nm) on a spectrofluorimeter plate-reader SpectraMax M5. The type of enzyme inhibition was determined graphically using the Lineweaver-Burk plot according to the equation (1).

$$1 / V = (K_m + [S]) / (V_{max} \times [S]) = (K_m / V_{max}) \times (1 / [S]) + (1 / V_{max}) \quad (1)$$

where V is the reaction velocity, V_{max} the maximum reaction velocity, K_m the Michaelis-Menten constant and [S] the substrate concentration.

The inhibition constant K_i was determined by a curve fitting using Graph Pad Prism software (La Jolla, USA) to the Dixon plot for non-competitive inhibition according to the equation (2).

$$1 / V = (1 / V_{max}) \times (1 + K_m / [S]) \times (1 + [I] / K_i) \quad (2)$$

where [I] is the inhibitor concentration.

The rate constant for association (k_{ass}) was determined by monitoring the time dependence of association of gingipains with the PDs. Enzymes (10 nM) were incubated at 37 °C with increasing concentrations of PD in the gingipain assay buffer supplemented with L-cysteine and residual enzymatic activity was measured as a function of time after addition of Z-Arg-AMC (50 μM). The k_{ass} was determined by non-linear regression plotting $[EI] = [E_0] - [E]$ against time (Graph Pad Prism software, La Jolla, USA).

The dissociation rate constant (k_{diss}) was calculated from the experimental values of K_i and k_{ass} according to the equation (3).

$$k_{diss} = K_i \times k_{ass} \quad (3)$$

2.7. Visualisation of the complex formation by native gel and western blot

Two µg of RgpB or Kgp catalytic domain were incubated for 15 min with the PDs at a molar ratio 1:1 in assay buffer with or without 50 mM L-cysteine supplementation. The samples were then electrophoresed for 3 hours at 20 mA on a 12% Native-PAGE gel and stained with SimplyBlue SafeStain (Invitrogen). Alternatively, resolved proteins were electrotransferred onto nitrocellulose membrane (1 hour at 100 V) and non-specific binding sites blocked with a 5% skim milk solution. Membranes were then incubated with rabbit pAbs anti-RgpB or a mouse mAbs anti-Kgp followed by the corresponding secondary antibodies anti-rabbit IgG-peroxidase conjugate and anti-mouse IgG-alkaline phosphatase conjugate (both from Sigma). Proteins of interest were visualized with TMB Membrane Peroxidase Substrate (KPL) or with AP Conjugate Substrate Kit (BioRad), respectively.

In some experiments, RgpB was pre-incubated for 15 min in the assay buffer supplemented with 5 mM L-cysteine with various irreversible inhibitors (TLCK, FR-FMK, Z-FFR-CMK and YPR-CMK at 100 μM final concentration) before the addition of PD_{RgpB}. After 15 min incubation, the mixture was subjected to native PAGE or size exclusion chromatography (see below).

2.8. Size-exclusion chromatography studies of the complex forming capacity of PD_{RgpB} with its mature enzyme

RgpB (10 μM) and increasing concentrations of PD_{RgpB} (10, 20 and 40 μM final concentration) were incubated together or separately for 15 min at room temperature in gel filtration buffer (50 mM Phosphate Buffer, 0.15 M NaCl, pH 7.2) with or without 5 mM L-cysteine. The mixture (100 μl) was then resolved by size-exclusion chromatography on Superdex^{TM} 200 10/300 GL (GE Healthcare) using an AKTA purifier 900 FPLC system (GE Healthcare) at a flow rate of 0.25 ml/min. Elution profile was followed at 280 nm and 0.5 ml fractions were collected. The calibration profile of the column was obtained using the Gel Filtration Calibration Kits LMW and HMW (GE Healthcare) following the manufacturer's instructions (Protein standards: aprotinin, 6.5 kDA; ribonuclease A, 13.7 kDa; carbonic anhydrase, 29 kDa; ovalbumin, 44 kDa; conalbumin, 75 kDa; aldolase, 158 kDa; and ferritin, 440 kDa). Thirty μl samples of each fraction were incubated 10 min in the presence of 5 mM TLCK, resolved by SDS-PAGE on a 4-12% Bis-Tris gel (Invitrogen) and then stained with SimplyBlue SafeStain (Invitrogen).

2.9. Stability of the RgpB-PD_{RgpB} complex

RgpB (2 μM) was incubated with its PD at different concentrations (10, 20, and 40 μM final) at room temperature in the assay buffer supplemented with 10 mM L-cysteine. As a control, RgpB was pre-incubated with 5 mM TLCK before PD incubation under the same condition above. At various time points (t = 0, 2, 5, 24, 48, 72, 96 h), aliquots were removed and residual activity of RgpB was determined using L-BAPNA as described previously. At the same time points, aliquots were withdrawn, treated with 5 mM TLCK and then subjected to SDS-PAGE on 4-12 % Bis-Tris gel (Invitrogen) and stained with SimplyBlue SafeStain to visualize PD degradation. Alternatively, SDS-PAGE resolved proteins were electrotransferred onto a PVDF membrane for N-terminal sequence analysis of the main discrete degradation product(s). In parallel, to monitor the presence of the residual complex, aliquots of samples equivalent to 2 μg of RgpB were resolved by Native-PAGE using 12% gels.

2.10. Bacteria cultivation and characterization

Porphyromonas gingivalis strains were grown in enriched tryptic soy broth (eTSB) (30 g/L Trypticase soy broth, 5 g/L yeast extract, 5 mg/L hemin, 2 mg/L menadione supplemented with 5 mM L-cysteine, pH 7.5) in an anaerobic chamber (Bactron IV; Sheldon Manufacturing Inc., OR) in an atmosphere of 90% N_2, 5% CO_2, and 5% H_2. Cultures cultivated into the stationary phase of growth were adjusted to the same OD_{600} 1.5 and centrifuged at 5,000 × g for 10 min. Supernatants were collected and pellets were washed and resuspended in PBS to the original volume to obtain the cells fraction. In supernatants and cell suspensions, the presence of RgpB was determined by Western-blotting with specific rabbit pAbs anti-RgpB while the gingipain activity was measured at 37 °C using L-BAPNA substrate as described earlier.

2.11. Inhibition of different cellular forms of RgpB by PD

Whole cultures of *P. gingivalis* strains W83, HG66, RgpA-C and RgpB-6HTSI were grown to early stationary phase and the cellular fraction was separated from the cell-free media by centrifugation as above. Washed bacterial cell suspension or cell-free culture media were incubated at 37 °C in assay buffer supplemented with 10 mM L-cysteine in the presence of increasing concentrations of PD_{RgpB} (0.1 nM to 10 μM) in a 96-well plate. In each case, cultures or culture-derived fractions were adjusted to have Rgp activity equivalent to 10 nM of purified

RgpB. After 15 min, the residual gingipain activity was determined using L-BAPNA as the substrate. The IC_{50} was determined using Graph Pad Prism software.

3. Results

3.1. Rgps, but not Kgp, are inhibited by N-terminal prodomain

We have previously shown that when expressed in yeast, proRgpB rapidly undergoes autoproteolytic processing at the N- and C-termini to yield fully active enzyme. Therefore, we have concluded that N-terminal prodomain (PD) allows low level of latency to proRgpB [39]. To revisit the role of the PD in the control of gingipain activity, we used recombinant PDs derived from RgpA, RgpB, and Kgp to investigate their interactions with the mature proteases (Fig. S1). All three PDs are approximately 23 kDa in mass with 203-205 residues in length. There is 75% identity between PD derived from RgpA (PD_{RgpA}) and PD derived from RgpB (PD_{RgpB}) but only 20% identity with PD derived from Kgp (PD_{Kgp}) – this is reflected in their pI's of 9.47, 8.06 and 5.95, respectively. As shown in Fig. 1, amidolytic, aminopeptidase and proteolytic activities of RgpA and RgpB (at 10 nM concentration) were efficiently cross-inhibited by their PDs with IC_{50} in the range from 4.5 nM to 23.7 nM (Table I). Comparison of the IC_{50} values suggests that RgpA was slightly more sensitive to inhibition by the Rgps-derived PDs than RgpB. In contrast, PDs originated from Rgps had limited effect on Kgp proteolytic and amidolytic activities (IC_{50} in the range 7.9 μM to >100 μM). Surprisingly, Kgp-derived PD (PD_{Kgp}) up to 1,000-fold excess did not interfere with the activity of any gingipain, including Kgp. This result suggests that PD from Rgps and Kgp may play different function in the maturation of progingipains, as reflected in their differing pI's.

3.2. RgpB forms stable stoichiometric inhibitory complexes with profragments

To further investigate PD interaction with RgpB, we assessed complex stability and reaction stoichiometry by native PAGE. A complex formed by equimolar concentration of the negatively charged RgpB CD (pI 4.95) and the cationic PD_{RgpB} (pI 8.06) migrated with significantly slower electrophoretic mobility than free RgpB. Of note, PD_{RgpB} did not penetrate into the gel in native PAGE conditions due to its high pI. A shift of RgpB-PD_{RgpB} complex to a lower mobility band was confirmed by Western blot analysis (Fig. 2A). Conversely, no complex formation was detected between RgpB and PD_{Kgp} (Fig. 2B), Kgp and PD_{RgpB} (Fig. 2C), Kgp and PD_{Kgp} (Fig.

2D). This correlates with the lack of RgpB inhibition by PD_{Kgp} through enzymatic analysis and very weak if any inhibition of Kgp by PD_{RgpB} or PD_{Kgp} (Fig. 1, Table 1).

Formation of the 1:1 stoichiometric complex between RgpB and its PD was confirmed by size exclusion chromatography. At a slight molar excess of PD_{RgpB} to RgpB and in the presence of L-cysteine, a peak containing both proteins was eluted from the Superdex 200 column at the volume equivalent to the molecular mass of the complex (62 kDa) (Fig. 3AB). By contrast, in the absence of cysteine, even at four molar excess of PD_{RgpB}, a portion of RgpB did not form the complex. This is apparently due to reversible modification of cysteine residue(s) in RgpB with dithiodipyridine used during gingipain purification.

Finally, the stability of the complex was tested by incubation of the proformed complex at room temperature. At 5 molar excess of PD_{RgpB} over RgpB, no gingipain activity was released up to 96h incubation despite the clear decrease of intensity of a band corresponding to PD_{RgpB} in SDS-PAGE (Fig. 4A). The apparent reduction of molecular mass of PD was due to cleavage at the N-terminus of the PD (GPLGSQPAER#GRN….). The truncation, however, did not affect the complex stability as shown by native PAGE (Fig. 4B). The depletion of PD and time-dependent truncation was also observed in the complex formed with the large excess of PD. This suggests that RgpB in the complex retains some *in trans* activity responsible for degradation of the excess of free PD and truncation of the PD in the complex but is unable to degrade attached PD in *cis* and escape from the inhibitory complex.

Collectively these results indicate that PDs derived from RgpA and RgpB form very stable 1:1 stoichiometric inhibitory complexes with their cognate mature gingipains only. Therefore they can prevent premature release of gingipain activity in the *P. gingivalis* periplasm.

3.3. Profragments are non-competitive reversible inhibitors of the mature gingipains

To determine the mode of inhibition, we performed a kinetic analysis of RgpB and HRgpA interaction with their PDs. The inhibition followed the Michaelis-Menten kinetic and was dependent on the concentration of PD and the substrate concentration (Fig. 5AB) indicating the reversible mode of inhibition. This was confirmed by re-plotting the kinetic data using the Lineweaver-Burk equation, which revealed the formation of non-competitive, reversible inhibitory complexes (Fig. 5CD). Finally, the steady-state inhibition constant (K_i) was determined graphically using the Dixon plot for non-competitive inhibition (Fig. 5EF). The results of kinetic analysis of inhibition (K_i, k_{ass}, and k_{dis}) are summarized in Table 2 showing that PDs are very efficient, low nanomolar inhibitors of mature gingipains with K_i in the range from 0.85 to 6.2 nM.

In concordance with IC_{50} values (Table 1), HRgpA was more efficiently inhibited by PDs than RgpB.

3.4. Rgps inhibition by PDs depends on Arg^{102}

Alignment of gingipain prodomain sequences revealed a conservation of Arg or Lys residues at (RgpB-equivalent) positions 66, 102 and 159 in PD_{Rgps} and PD_{Kgp}, respectively (Fig. S1). In consideration of each gingipain's specificity, we hypothesized that one of these conserved residue functions as the P1 inhibitory residue of the profragments. To verify this hypothesis, we have expressed PD_{RgpB} with the following mutations: R66K, R66A, R102K, R102A, R102E, R102Q and R159K. As shown in Table 3, mutation of Arg-102 had a strong impact on the inhibitory activity of PD_{RgpB}. While the R102K mutant exhibited a one log reduced efficiency to inhibit RgpB, Arg-102 substitution with Ala, Glu, Gln totally abolished its inhibitory activity. In contrast, mutations of other Arg residues had relatively low (R66K) or no effect (R66K and R159K) on the PD inhibitory property. Significantly, none of Arg to Lys mutation converted PD_{RgpB} into even a weak inhibitor of Kgp (data not shown). The CD spectra analysis of mutated PDs was found to be identical to the spectrum of the native PD with the exception of the R66K variant showing some increase in α-helix content at the expense of β-sheet content (Fig. S2). This suggests the observed decrease in inhibitory capacity of R66K is most likely due to some minor structural changes. Together, these results strongly implicate Arg-102 as the P1 residue in the inhibitory interaction between PD and Rgps. This is in agreement with a previous observation of PD_{RgpB} cleavage at Arg-102 during the activation/maturation process of recombinant proRgpB expressed in yeast cells [39].

3.5. The stable complex formation occurs via profragment interaction independent of the catalytic cysteine residue

Dependence of the PD_{RgpB}-RgpB complex formation on the pretreatment of RgpB with reducing agents (Fig. 1) and reversible abrogation of the interaction with a cysteine-modifying reagent dithiodipyridine (data not shown), suggests that the reduced catalytic Cys449 is essential for inhibitory interactions. Unexpectedly, however, we found that pretreatment of RgpB with an irreversible inhibitor (TLCK) to covalently modify Cys449 did not affect the inhibitory complex formation as assessed by gel filtration, native PAGE and Western blotting (Fig. 6). Similarly, blocking the RgpB catalytic cysteine with FR-FMK had no significant effect

on the interaction between RgpB and PD_{RgpB}. In stark contrast, however, pretreatment of RgpB with chloromethylketone inhibitors carrying three amino acid residues (Z-FFR-CMK and YPR-CMK), strongly interfered with the complex formation. As shown by gel filtration, RgpB inactivated by these chloromethylketones was eluted predominantly as the free enzyme accompanied by a small amount of the complex (Fig. 6A). The minimal complex formation between Z-FFR-CMK and YPR-CMK-treated RgpB and PD_{RgpB} was confirmed by native PAGE (Fig. 6B). Together, these findings argue that interaction with the catalytic Cys449 is not involved in complex formation. Conversely, the presence of the P3 and P2 residues of the tripeptide inhibitors interfering with the complex formation suggests PD_{RgpB} inhibits RgpB through interactions with non-primed substrate binding subsites on the protease moiety.

The lack of engagement of Cys449 in the RgpB inhibition by PD is compatible with the non-competitive mechanism of inhibition observed using Z-Arg-AMC as the substrate (Fig. 5). However, the strong interference with PD_{RgpB}-RgpB complex formation by covalent inhibitors with three amino acid residues suggests that the inhibition mode would be different if RgpB residual activity is assayed using longer substrates interacting with S2 and S3 binding subsites. To verify this contention, we re-analyzed the kinetics of RgpB inhibition by PD_{RgpB} using Z-FR-AMC, Z-GPR-AMC and Z-AGPR-AMC as the substrates. In agreement with the prediction, the mode of inhibition shifted from non-competitive to partially competitive inhibition, the latter especially evident with the longest substrate (Fig. 7).

3.6. Prodomain weakly inhibits cell-associated or glycosylated forms of gingipains

Rgps occurs in different forms, including highly glycosylated cell-associated RgpB (membrane-type RgpB; mt-RgpB), RgpA-Kgp complex on the cell surface and soluble enzymes released into the culture media. To assess how these forms interact with PD_{RgpB}, we have determined IC_{50} of inhibition of Rgps in whole cultures and cell-free culture media of different *P. gingivalis* strains. Of note, in all cases, Rgp activity was adjusted to be equivalent to 10 nM concentration of the purified, active-site titrated RgpB. As a control to evaluate the effect of growth media and bacterial cells on gingipain interaction with PD_{RgpB}, purified RgpB was spiked into sterile medium and subcellular fractions (whole culture, cell-free culture supernatant, and washed cells) derived from the culture of a gingipain-null strain. Regardless of the strain, soluble, non-glycosylated Rgps in cell-free culture media were inhibited with the same potency as the purified enzyme (IC_{50} in the range from 0.011 to 0.022 μM) (Table 4). However, in the presence of bacterial cells (whole cultures of strains secreting non-glycosylated gingipains into

the media or spiked with purified RgpB) the IC_{50} of inhibition was increased by one log (in the range from 0.116 to 0.128 μM). This decrease in potency of Rgps inhibition by PD_{RgpB} in the presence of *P. gingivalis* cells was not due to PD_{RgpB} binding to or being degraded by the bacterial cells because the level of recovered PD_{RgpB} in the supernatant remained constant after the cells were removed by centrifugation (Fig. S3). Finally, cell-associated Rgps were fairly resistant to inhibition by PD_{RgpB} (IC_{50} > 1 μM). This resistance is partly dependent on gingipain glycosylation since purified, membrane-type highly glycosylated RgpB was still five times more susceptible to inhibition by PD_{RgpB} (IC_{50} = 0.188 μM) than cell-associated enzyme (Table 4). Collectively, these results suggest that once Rgps are secreted, PD cleavage in the context of *P. gingivalis* cells will lead to dissociation of the PD from the complex to release active gingipains into the extracellular environment. Of note, recombinant PD_{RgpB} added to the culture medium had no effect on *P. gingivalis* growth (Fig. S4).

4. Discussion

In prokaryotes and eukaryotes, amino-terminal prodomains of enzymes are commonly observed to exert temporal and/or spatial control over proteolytic activity to maintain latency of secreted proteases [1, 40]. Prodomains have also been reported to play the role of tethered chaperones assisting protein folding *in cis* [41, 42]. Inhibition of cysteine proteases by PDs is accomplished in several different ways. In lysosomal cathepsins (family C1 of cysteine proteases), a C-terminal segment of a structurally related PD binds in an extended conformation covering the entire active site cleft in an opposite orientation to that of substrate binding [43]. In staphopain A (family C47) of *Staphylococcus aureus*, PD also binds in the opposite orientation to substrates, but occludes only the primed sites in the active site cleft of the protease [8]. Conversely, in *Streptococcus pyogenes* streptopain (SpeB) and *Prevotella intermedia* interpain A, both belonging to family C10, the mechanism of latency relies on displacement of the histidine residue of the catalytic dyad by structurally unique PDs [5, 9]. Here, we have characterized the kinetics of inhibitory interaction of gingipain-derived recombinant PDs with mature gingipains.

Recombinant RgpA- and RgpB-derived PDs are tight-binding inhibitors of Rgp's with K_i in the low nanomolar range. This resembles interaction between lysosomal cathepsins and their PDs (K_i in the range from 0.0059 to 5.6 nM) [2]. On the other hand, while cathepsins-derived PDs are non-competitive inhibitors [44, 45], the inhibition of Rgps is of the competitive type, at least with Z-Arg-AMC and Z-FR-AMC as substrates. Interestingly, the mode of inhibition of

RgpB by PD_{RgpB} is changed to the mixed inhibition type when tri- and tetrapeptide-substrates are used to measure the gingipain residual activity suggesting that longer substrates are less likely to compete with PD for the substrate-binding cleft. This is corroborated by the finding that pretreatment of RgpB with irreversible active-site inhibitors, which covalently bind to catalytic Cys244 Sγ through methylene group [46], variably affected formation of the RgpB-PD_{RgpB} complex. While TLCK and FR-FMK exerted no effect on stable complex formation, tripeptidyl inhibitors YPR-CMK and Z-FFR-CMK entirely blocked the interaction. As similar interaction must take place during PD_{RgpB} interaction with FR-FMK pretreated RgpB and the Arg residue of covalently bound FR-FMK must be replaced by Arg-102 to allow for stable complex formation. This is apparent from the finding that R102A, R102E and R102Q mutants of PD have no inhibitory activity while conservative replacement of Arg-102 with Lys reduces PD_{RgpB} affinity by one log. Directed mutagenesis of other conserved Arg residues had no effect on inhibitory activity of PD_{RgpB}. In the case of longer inhibitors, additional interactions of P3 and P4 residues (carboxybenzyl group of Z-FFR-CMK) with substrate binding subsites may prevent insertion of PD_{RgpB} Arg-102 into the S1 pocket and therefore destabilize the inhibitory complex. Similarly, reversible modification of Cys-244 Sγ by dithiodipyridine must somehow block this interaction between PD_{RgpB} and the enzyme since it is clear from the complex structure that no other Cys residue are in the spatial position to interfere with complex formation.

Rgps-derived PD very weakly inhibited Kgp (IC_{50} around 10 μM) and replacement of Arg-102 with lysine residue to match the Kgp specificity did not change efficiency of the inhibition. Furthermore, recombinant PD_{Kgp} has absolutely no inhibitory activity if supplied *in trans* despite the latency of proKgp (data not shown). It can be speculated that PD_{Kgp} functions only in *cis* as observed for inhibition of staphopains, interpain A, and streptopain (SpeB) by their PDs [5, 8, 9]. Alternatively, the Kgp latency may be dependent on the C-terminal extension while PD_{Kgp} has a different function as described for PDs of other cysteine and serine proteases, such as an intramolecular chaperone.

Previously, we have found that the full-length RgpB zymogen expressed in *Saccharomyces cerevisiae* strain YG227 rapidly auto-processed itself via an intermolecular mechanism (where a different catalytic site attacks the bonds in an adjacent molecule). Based on the analysis of the processing, we concluded that the N-terminal PD and C-terminal extension render a low amount of latency and the zymogen was substantially active [39]. This conclusion is in conflict with numerous reports showing that *P. gingivalis* strains deficient in the PorSS secretion system accumulate in the periplasm large amounts of proteolytically inactive full-length and partially processed progingipains, including proRgpB [21, 27-31, 47, 48]. In the recombinant proRgpB,

high susceptibility of Arg^{102}-Ala to intermolecular hydrolysis suggests exposure of this region of the structure on the zymogen surface, possibly due to incomplete folding of the prodomain in the yeast system.

The latency of proRgpB is apparently very tight since the RgpB-PD_{RgpB} complex *in trans* shows extraordinary stability. No release of inhibition of RgpB activity was seen even after 5 days of incubation of the complex at room temperature. This suggests the presence of a mechanism releasing PD after progingipains are transported from the periplasm across the outer membrane to the bacterial surface. In eukaryotic cells, disruption of propeptide-mature enzyme interaction leading to activation of procathepsin is accomplished by change of pH in specific subcellular compartments and is facilitated by glycosaminoglycans [43, 49]. Bacteria, however, do not have subcellular compartments with different pH. Nevertheless, based on the present knowledge, we can envision the following mechanism. Interaction of progingipains with the PorSS translocon [21] induces structural changes facilitating autocatalytic intra- or interproteolytic cleavage at the Arg^{102}-Ala peptide bond. Sequential autoproteolytic cleavage at Arg^{225}-Tyr removes the remainder of the PD_{RgpB} which is subsequently degraded. Concurrently or subsequent to the autoprocessing at the N-terminus, a designated C-terminal signal peptidase of the PorSS system (PG0026) located on the cell surface removes the C-terminal domain (CTD) of RgpB [48] and the mature protease is either glycosylated to be retained on the bacterial surface or released as a soluble form into the growth medium. In any case, failure of PD_{RgpB} to efficiently inhibit cell-associated Rgps (Table 4) argues that a mechanism exist to release active gingipains from the complex outside the cell, thus, protecting the periplasm against potentially deleterious effect of prematurely activated enzymes.

Acknowledgments

This study was supported in part by grants from European, US American, Polish, Spanish, and Catalan agencies (UMO-2012/04/A/NZ1/00051, 2011/03/N/NZ1/00586, 2137/7.PR-EU/2011/2, DE09761, FP7-HEALTH-F3-2009-223101 “AntiPathoGN”; FP7-HEALTH-2010-261460 “Gums&Joints”; FP7-PEOPLE-2011-ITN-290246 “RAPID”; BIO2009-10334; BFU2012-32862; CSD2006-00015; Fundació “La Marató de TV3” grant 2009-100732; and 2009SGR1036).

Appendix A. Supplementary data

Supplementary data to this article can be found online at XXX

References

[1] A.R. Khan, M.N. James, Molecular mechanisms for the conversion of zymogens to active proteolytic enzymes, Protein Sci, 7 (1998) 815-836.

[2] B. Wiederanders, G. Kaulmann, K. Schilling, Functions of propeptide parts in cysteine proteases, Curr Protein Pept Sci, 4 (2003) 309-326.

[3] J. Potempa, E. Golonka, R. Filipek, L.N. Shaw, Fighting an enemy within: cytoplasmic inhibitors of bacterial cysteine proteases, Mol Microbiol, 57 (2005) 605-610.

[4] A.V. Serkina, T.F. Gorozhankina, A.B. Shevelev, G.G. Chestukhina, Propeptide of the metalloprotease of Brevibacillus brevis 7882 is a strong inhibitor of the mature enzyme, FEBS Lett, 456 (1999) 215-219.

[5] T.F. Kagawa, J.C. Cooney, H.M. Baker, S. McSweeney, M. Liu, S. Gubba, J.M. Musser, E.N. Baker, Crystal structure of the zymogen form of the group A Streptococcus virulence factor SpeB: an integrin-binding cysteine protease, Proc Natl Acad Sci U S A, 97 (2000) 2235-2240.

[6] P. Braun, W. Bitter, J. Tommassen, Activation of Pseudomonas aeruginosa elastase in Pseudomonas putida by triggering dissociation of the propeptide-enzyme complex, Microbiology, 146 (Pt 10) (2000) 2565-2572.

[7] K. Ponnuraj, S. Rowland, C. Nessi, P. Setlow, M.J. Jedrzejas, Crystal structure of a novel germination protease from spores of Bacillus megaterium: structural arrangement and zymogen activation, J Mol Biol, 300 (2000) 1-10.

[8] R. Filipek, R. Szczepanowski, A. Sabat, J. Potempa, M. Bochtler, Prostaphopain B structure: a comparison of proregion-mediated and staphostatin-mediated protease inhibition, Biochemistry, 43 (2004) 14306-14315.

[9] N. Mallorqui-Fernandez, S.P. Manandhar, G. Mallorqui-Fernandez, I. Uson, K. Wawrzonek, T. Kantyka, M. Sola, I.B. Thogersen, J.J. Enghild, J. Potempa, F.X. Gomis-Ruth, A new autocatalytic activation mechanism for cysteine proteases revealed by Prevotella intermedia interpain A, J Biol Chem, 283 (2008) 2871-2882.

[10] M. Comellas-Bigler, K. Maskos, R. Huber, H. Oyama, K. Oda, W. Bode, 1.2 A crystal structure of the serine carboxyl proteinase pro-kumamolisin; structure of an intact pro-subtilase, Structure, 12 (2004) 1313-1323.

[11] T.Y. Gromova, I.V. Demidyuk, V.I. Kozlovskiy, I.P. Kuranova, S.V. Kostrov, Processing of protealysin precursor, Biochimie, 91 (2009) 639-645.

[12] Z. Huang, Y. Feng, D. Chen, X. Wu, S. Huang, X. Wang, X. Xiao, W. Li, N. Huang, L. Gu, G. Zhong, J. Chai, Structural basis for activation and inhibition of the secreted chlamydia protease CPAF, Cell Host Microbe, 4 (2008) 529-542.

[13] A. Ruggiero, D. Marasco, F. Squeglia, S. Soldini, E. Pedone, C. Pedone, R. Berisio, Structure and functional regulation of RipA, a mycobacterial enzyme essential for daughter cell separation, Structure, 18 (2010) 1184-1190.

[14] H.S. O'Neil, B.M. Forster, K.L. Roberts, A.J. Chambers, A.P. Bitar, H. Marquis, The propeptide of the metalloprotease of Listeria monocytogenes controls compartmentalization of the zymogen during intracellular infection, J Bacteriol, 191 (2009) 3594-3603.

[15] N.N. Nickerson, L. Prasad, L. Jacob, L.T. Delbaere, M.J. McGavin, Activation of the SspA serine protease zymogen of Staphylococcus aureus proceeds through unique variations of a trypsinogen-like mechanism and is dependent on both autocatalytic and metalloprotease-specific processing, J Biol Chem, 282 (2007) 34129-34138.

[16] N.N. Nickerson, V. Joag, M.J. McGavin, Rapid autocatalytic activation of the M4 metalloprotease aureolysin is controlled by a conserved N-terminal fungalysin-thermolysin-propeptide domain, Mol Microbiol, 69 (2008) 1530-1543.

[17] M.A. Curtis, J. Aduse-Opoku, M. Rangarajan, Cysteine proteases of Porphyromonas gingivalis, Crit Rev Oral Biol Med, 12 (2001) 192-216.

[18] M.A. Curtis, H.K. Kuramitsu, M. Lantz, F.L. Macrina, K. Nakayama, J. Potempa, E.C. Reynolds, J. Aduse-Opoku, Molecular genetics and nomenclature of proteases of Porphyromonas gingivalis, J Periodontal Res, 34 (1999) 464-472.

[19] Y. Guo, K.A. Nguyen, J. Potempa, Dichotomy of gingipains action as virulence factors: from cleaving substrates with the precision of a surgeon's knife to a meat chopper-like brutal degradation of proteins, Periodontol 2000, 54 (2010) 15-44.

[20] K. Nakayama, F. Yoshimura, T. Kadowaki, K. Yamamoto, Involvement of arginine-specific cysteine proteinase (Arg-gingipain) in fimbriation of Porphyromonas gingivalis, J Bacteriol, 178 (1996) 2818-2824.

[21] K. Sato, M. Naito, H. Yukitake, H. Hirakawa, M. Shoji, M.J. McBride, R.G. Rhodes, K. Nakayama, A protein secretion system linked to bacteroidete gliding motility and pathogenesis, Proc Natl Acad Sci U S A, 107 (2010) 276-281.

[22] K.A. Nguyen, J. Travis, J. Potempa, Does the importance of the C-terminal residues in the maturation of RgpB from Porphyromonas gingivalis reveal a novel mechanism for protein export in a subgroup of Gram-Negative bacteria?, J Bacteriol, 189 (2007) 833-843.

[23] J. Potempa, A. Sroka, T. Imamura, J. Travis, Gingipains, the major cysteine proteinases and virulence factors of Porphyromonas gingivalis: structure, function and assembly of multidomain protein complexes, Curr Protein Pept Sci, 4 (2003) 397-407.

[24] P.D. Veith, G.H. Talbo, N. Slakeski, S.G. Dashper, C. Moore, R.A. Paolini, E.C. Reynolds, Major outer membrane proteins and proteolytic processing of RgpA and Kgp of Porphyromonas gingivalis W50, Biochem J, 363 (2002) 105-115.

[25] N. Slakeski, P.S. Bhogal, N.M. O'Brien-Simpson, E.C. Reynolds, Characterization of a second cell-associated Arg-specific cysteine proteinase of Porphyromonas gingivalis and identification of an adhesin-binding motif involved in association of the prtR and prtK proteinases and adhesins into large complexes, Microbiology, 144 (Pt 6) (1998) 1583-1592.

[26] J. Potempa, R. Pike, J. Travis, The multiple forms of trypsin-like activity present in various strains of Porphyromonas gingivalis are due to the presence of either Arg-gingipain or Lys-gingipain, Infect Immun, 63 (1995) 1176-1182.

[27] K. Sato, H. Yukitake, Y. Narita, M. Shoji, M. Naito, K. Nakayama, Identification of Porphyromonas gingivalis proteins secreted by the Por secretion system, FEMS Microbiol Lett, 338 (2013) 68-76.

[28] K. Sato, E. Sakai, P.D. Veith, M. Shoji, Y. Kikuchi, H. Yukitake, N. Ohara, M. Naito, K. Okamoto, E.C. Reynolds, K. Nakayama, Identification of a new membrane-associated protein that influences transport/maturation of gingipains and adhesins of Porphyromonas gingivalis, J Biol Chem, 280 (2005) 8668-8677.

[29] K. Saiki, K. Konishi, The role of Sov protein in the secretion of gingipain protease virulence factors of Porphyromonas gingivalis, FEMS Microbiol Lett, 302 (2010) 166-174.

[30] K. Saiki, K. Konishi, Identification of a novel Porphyromonas gingivalis outer membrane protein, PG534, required for the production of active gingipains, FEMS Microbiol Lett, 310 (2010) 168-174.

[31] I. Ishiguro, K. Saiki, K. Konishi, PG27 is a novel membrane protein essential for a Porphyromonas gingivalis protease secretion system, FEMS Microbiol Lett, 292 (2009) 261-267.

[32] J. Potempa, K.A. Nguyen, Purification and characterization of gingipains, Curr Protoc Protein Sci, Chapter 21 (2007) Unit 21 20.

[33] P.D. Skottrup, P. Leonard, J.Z. Kaczmarek, F. Veillard, J.J. Enghild, R. O'Kennedy, A. Sroka, R.P. Clausen, J. Potempa, E. Riise, Diagnostic evaluation of a nanobody with picomolar affinity toward the protease RgpB from Porphyromonas gingivalis, Anal Biochem, 415 (2011) 158-167.

[34] M. Rangarajan, S.J. Smith, S. U, M.A. Curtis, Biochemical characterization of the arginine-specific proteases of Porphyromonas gingivalis W50 suggests a common precursor, Biochem J, 323 (Pt 3) (1997) 701-709.

[35] J. Potempa, K.A. Nguyen, Purification and characterization of gingipains, Curr Protoc Protein Sci, Chapter 21 (2007) Unit 21 20.

[36] P. Unneberg, J.J. Merelo, P. Chacon, F. Moran, SOMCD: method for evaluating protein secondary structure from UV circular dichroism spectra, Proteins, 42 (2001) 460-470.

[37] C. Cole, J.D. Barber, G.J. Barton, The Jpred 3 secondary structure prediction server, Nucleic Acids Res, 36 (2008) W197-201.

[38] F. Veillard, B. Potempa, M. Poreba, M. Drag, J. Potempa, Gingipain aminopeptidase activities in Porphyromonas gingivalis, Biol Chem, (2012).

[39] J. Mikolajczyk, K.M. Boatright, H.R. Stennicke, T. Nazif, J. Potempa, M. Bogyo, G.S. Salvesen, Sequential autolytic processing activates the zymogen of Arg-gingipain, J Biol Chem, 278 (2003) 10458-10464.

[40] C. Wandersman, Secretion, processing and activation of bacterial extracellular proteases, Mol Microbiol, 3 (1989) 1825-1831.

[41] M. Inouye, Intramolecular chaperone: the role of the pro-peptide in protein folding, Enzyme, 45 (1991) 314-321.

[42] P.N. Bryan, Prodomains and protein folding catalysis, Chem Rev, 102 (2002) 4805-4816.

[43] V. Turk, V. Stoka, O. Vasiljeva, M. Renko, T. Sun, B. Turk, D. Turk, Cysteine cathepsins: from structure, function and regulation to new frontiers, Biochim Biophys Acta, 1824 (2012) 68-88.

[44] T. Fox, E. de Miguel, J.S. Mort, A.C. Storer, Potent slow-binding inhibition of cathepsin B by its propeptide, Biochemistry, 31 (1992) 12571-12576.

[45] M. Cygler, J. Sivaraman, P. Grochulski, R. Coulombe, A.C. Storer, J.S. Mort, Structure of rat procathepsin B: model for inhibition of cysteine protease activity by the proregion, Structure, 4 (1996) 405-416.

[46] A. Eichinger, H.G. Beisel, U. Jacob, R. Huber, F.J. Medrano, A. Banbula, J. Potempa, J. Travis, W. Bode, Crystal structure of gingipain R: an Arg-specific bacterial cysteine proteinase with a caspase-like fold, Embo J, 18 (1999) 5453-5462.

[47] K. Saiki, K. Konishi, Identification of a Porphyromonas gingivalis novel protein sov required for the secretion of gingipains, Microbiol Immunol, 51 (2007) 483-491.

[48] M.D. Glew, P.D. Veith, B. Peng, Y.Y. Chen, D.G. Gorasia, Q. Yang, N. Slakeski, D. Chen, C. Moore, S. Crawford, E.C. Reynolds, PG0026 is the C-terminal signal peptidase of a novel secretion system of Porphyromonas gingivalis, J Biol Chem, 287 (2012) 24605-24617.

[49] D. Caglic, J.R. Pungercar, G. Pejler, V. Turk, B. Turk, Glycosaminoglycans facilitate procathepsin B activation through disruption of propeptide-mature enzyme interactions, J Biol Chem, 282 (2007) 33076-33085.

Figure legend

Figure 1. Dose-dependant inhibition of gingipains activity by their prodomains

RgpB (open square), HRgpA (full square) and Kgp (full triangle) at 10 nM final concentration were incubated at 37 °C in assay buffer in the presence of increasing concentrations of PD_{RgpB}, PD_{RgpA} or PD_{Kgp}. After 15 mins, (**A**) residual amidolytic was determined using L-BAPNA for Rgps and Ac-Lys-pNA for Kgp; (**B**) residual aminopeptidase was determined using H-Arg-AMC (Rgps only) and (**C**) residual proteolytic activity determined using Azocoll.

Figure 2. Analysis of the complex formation between gingipains and their PDs by native-PAGE.

Gingipains were incubated for 15 min alone or with PDs at a molar ratio 1:1 in the assay buffer with or without 5 mM L-cysteine. Samples were then resolved by native-PAGE and stained with SimplyBlue SafeStain. Alternatively, resolved proteins were electrotransferred onto nitrocellulose membrane and analysed by Western blotting using anti-RgpB or anti-Kgp antibodies. (**A**) RgpB + PD_{RgpB}, (**B**) RgpB + PD_{Kgp}, (**C**) Kgp catalytic domain + PD_{RgpB}, and (**D**) Kgp catalytic domain + PD_{Kgp}. Due to its high pI, PD_{RgpB} did not penetrate into the gel in native PAGE conditions.

Figure 3. Analysis of the complex formation between RgpB and PD_{RgpB} by size-exclusion chromatography

RgpB (10 μM) and increasing concentration of PD_{RgpB} (10-, 20-, and 40 μM) were incubated together or separately for 15 min at room temperature in the presence or absence of 5 mM L-cysteine. (**A**) The mixture (100 μl) was subjected to a size-exclusion chromatography on Superdex^{TM} 200 10/300 to determine the molecular mass of the complex as compared to molecular mass standards (uppermost scale). Green, blue and red lines show elution profiles of PD_{RgpB}, RgpB, and the mixture of PD_{RgpB} with RgpB, respectively. (**B**) Aliquot of each collected fraction was subjected to SDS-PAGE to detect eluted proteins. Gels were stained SimplyBlue SafeStain.

Figure 4. Stability of the RgpB-PD_{RgpB} complex

PD (2 μg) was incubated with RgpB at 1:5, 1:10, and 1:20 molar ratios enzyme to PD at room temperature in the assay buffer supplemented with 10 mM L-cysteine. At defined time points (t

= 0-, 2-, 5-, 24-, 48-, 72-, 96 h) aliquots were removed and resolved by SDS-PAGE (**A**) and native PAGE (**B**). As a control (Ctl), PD was incubated in the same condition for 96 h with RgpB pretreated with 5 mM TLCK at the indicated molar ratios. Gels were stained with SimplyBlue SafeStain.

Figure 5. Steady-state kinetic of RgpB and HRgpA inhibition by their respective PDs. One nanomolar RgpB (**A, C** and **E**) and HRgpA (**B, D** and **F**) were incubated in a 96-well plate at 37 °C in assay buffer supplemented with 10 mM L-cysteine in the presence of increasing concentrations (from 0 to 10 nM) of PD_{RgpB} and PD_{RgpA}, respectively. After 15 min incubation, the residual gingipain activity was determined using several different concentrations (from 0 to 30 μM) of Z-Arg-AMC. (**A** and **B)** Michaelis-Menten plot of the rate of substrate hydrolysis; (**C** and **D)** Lineweaver-Burk plot of reciprocal initial velocity (V_o) versus reciprocal substrate concentration [S] to determine the type of inhibition; and (**E** and **F)** Dixon plot of reciprocal initial velocity (V_o) versus PD concentration to calculate the K_i value.

Figure 6. Effect of covalent irreversible inhibitors on RgpB-PD complex formation. RgpB (10 μM) was pre-incubated with TLCK, Z-FR-FMK, H-D-FFR-CMK, and YPR-CMK (each at 100 μM) in reducing buffer before equimolar amount of PD_{RgpB} was added. After 15-20 min incubation, samples were subjected to (**A**) size-exclusion chromatography on Superdex^{TM} 200 10/300 GL; (**B**) native PAGE followed by (**C**) Western blot analysis using anti-RgpB antibody.

Figure 7. The effect of the substrate structure on the mode of inhibition of RgpB by PD_{RgpB}. The mode of inhibition was determined graphically using the Lineweaver-Burk plot as described in Figure 3. Substrates used: (**A**) Z-FR-AMC, (**B**) Z-GPR-AMC and (**C**) Z-AGPR-AMC.

Appendices

Fig. A.1. Characteristics of gingipain prodomains

A) Sequences of PD_{RgpB}, PD_{HRgpA} and PD_{Kgp} were aligned using the ClustalW software. The secondary-structure content and localization were predicted using Jpred 3 (Cole C et al, Nucleic Acids Res, 2008); red shading represents α-helix prediction; yellow represents β-sheet prediction. **B)** Recombinant PDs fused to GST tag were expressed in *E. coli* and purified by affinity chromatography on GST-Sepharose column and the tags removed by Precission® protease. Five µg of recombinant proteins were resolved by SDS-PAGE (4-12% Bis-Tris gel) and stained with SimplyBlue™ SafeStain. **C)** CD of PD_{RgpA} (●), PD_{Kgp} (△), and PD_{RgpB} (○). **D)** Comparison of residues numbers, molecular mass, pI, shared percentage of identity of primary structure and the content of secondary structure elements theoretical vs. calculated from CD spectra.

Fig. A.2. CD spectra analysis of PD_{RgpB} mutants

CD spectra were obtained as described in Fig. S1. The table below the graph compares the content of α-helix and β-sheet in individual mutants of PD.

Fig. A.3. PD is neither degraded nor adsorbed on *P. gingivalis* cells. PD at two different concentrations was added to PBS (-) or to suspension of washed *P. gingivalis* Δ*rgpA*Δ*rgpB* cells (+). After incubation cells were removed by centrifugation and the presence of PD in supernatant determined by SDS-PAGE analysis.

Fig. A4. Effect of PDs on *P. gingivalis* growth

P. gingivalis W83 cultures at an early stationary phase were adjusted to $OD_{600\ nm}$ = 0.2 in eTSB media alone, complemented with PDs at 1 µM or with TLCK at 5 µM. The growth of the bacteria in anaerobic condition was then followed by measurements of $OD_{600\ nm}$.

Table 1

IC_{50} of inhibition of amidolytic (L-BAPNA and Ac-Lys-pNA), aminopeptidase (H-Arg-AMC) and proteolytic activities of gingipains by PDs.

Enzyme	Substrate	PD_{RgpB}	PD_{HRgpA}	PD_{Kgp}
RgpB	L-BAPNA	23.7 nM	15.7 nM	n.i.
	H-Arg-AMC	7.2 nM	6.9 nM	n.i.
	Azocoll	7.1 nM	7.3 nM	n.i.
HRgpA	L-BAPNA	12.6 nM	9.6 nM	n.i.
	H-Arg-AMC	4.9 nM	4.5 nM	n.i.
	Azocoll	5.8 nM	5.3 nM	n.i.
Kgp[(a)]	Ac-Lys-pNA	>100 μM	>100 μM	n.i.
	Azocoll	7.9 μM	13.9 μM	n.i.

n.i. – no inhibition

[(a)] PDs in the final concentration range from 1 μM to 200 μM were used to determine IC_{50} of Kgp inhibition.

Table 2

Kinetic parameters of gingipain inhibition by PDs.

PDs	Enzymes						
	RgpB			HRgpA			Kgp
	K_i (nM)	k_{ass} ($M^{-1}.s^{-1}$)	k_{diss} (s^{-1})	K_i (nM)	k_{ass} ($M^{-1}.s^{-1}$)	k_{diss} (s^{-1})	K_i (nM)
PD_{RgpB}	6.2 +/- 0.3	5016 +/- 95	3.1×10^{-5}	5.3 +/- 0.3	7545 +/- 85	4×10^{-5}	> 5000
PD_{RgpA}	2.1 +/- 0.2	6072 +/- 176	1.3×10^{-5}	0.85 +/- 0.1	7805 +/- 342	0.7×10^{-5}	> 5000
PD_{Kgp}	n.i.	-	-	n.i.	-	-	n.i.

n = 3 +/- SD

Table 3

Inhibition constant of RgpB interaction with PD mutants.

PD_{RgpB} mutant	K_i (nM)
Native	6.2 +/- 0.3
R66K	31 +/- 3.2
R66A	4.9 +/- 0.4
R102K	45.6 +/- 3
R102A	> 5000
R102E	> 5000
R102Q	> 5000
R159K	7.7 +/- 1.1

n = 3 +/- SD

Table 4

Comparison of PD_{RgpB} efficiency to inhibit different forms of Rgps.

Strain/fraction description	IC_{50} (μM)
W83 (whole culture, 90% Rgp activity cell-associated)	**1.457**
W83 Δ*rgpA* (whole culture, 80% RgpB activity cell associated)	**1.022**
W83 Δ*rgpA rgpB*-6HTSI (whole culture, all RgpB activity released in soluble, non-glycosylated form into media)	**0.113**
W83 Δ*rgpA rgpB*-6HTSI (cell-free culture medium)	**0.013**
HG66 (whole culture, all gingipain activity released in soluble, non-glycosylated form into media)	**0.116**
HG66 (cell-free culture medium)	**0.012**
RgpB + HG66 (Suspension of washed in PBS cells)	**0.122**
RgpB + W83 Δ*rgpA*Δ*rgpB*Δ*kgp* (whole culture)	**0.135**
RgpB + W83 Δ*rgpA*Δ*rgpB*Δ*kgp* (cell-free supernatant of culture media)	**0.022**
RgpB + W83 Δ*rgpA*Δ*rgpB*Δ*kgp* (suspension of bacterial cells washed in PBS)	**0.128**
RgpB (purified non-glycosylated)	**0.015**
mt-RgpB (purified)	**0.188**

n = 3

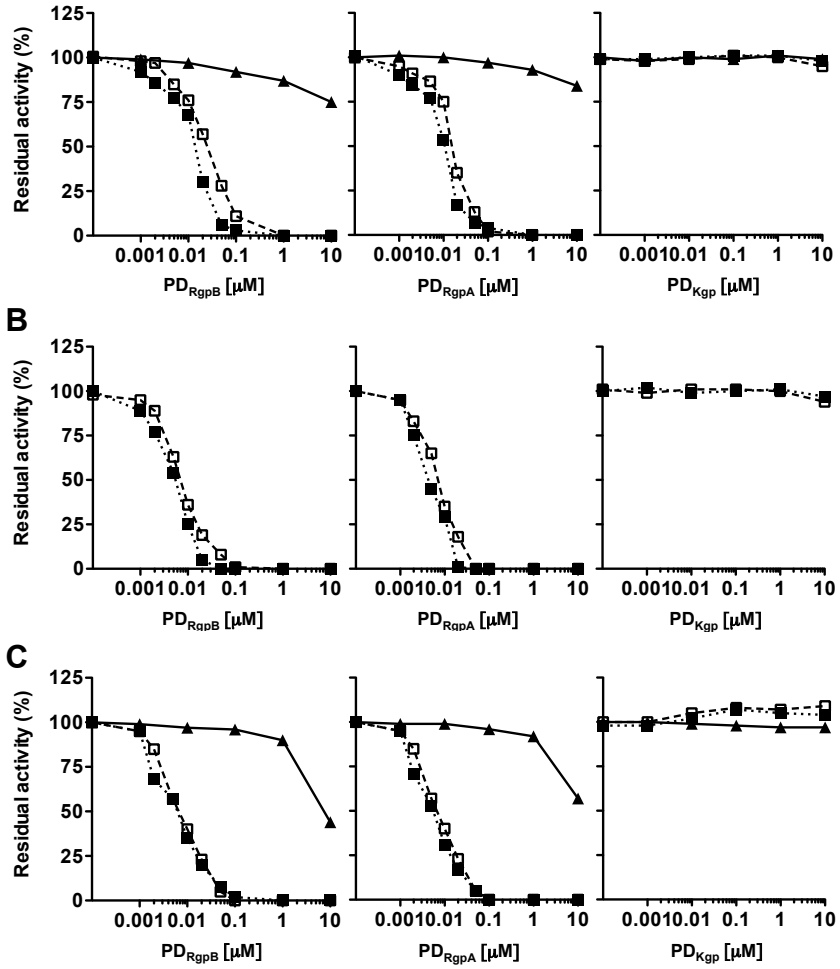
B
C
Residual activity (%)
125
100
75
50
25
0
0.001 0.01 0.1 1 10
PD$_{RgpB}$ [μM]
PD$_{RgpA}$ [μM]
PD$_{Kgp}$ [μM]

Figure 1

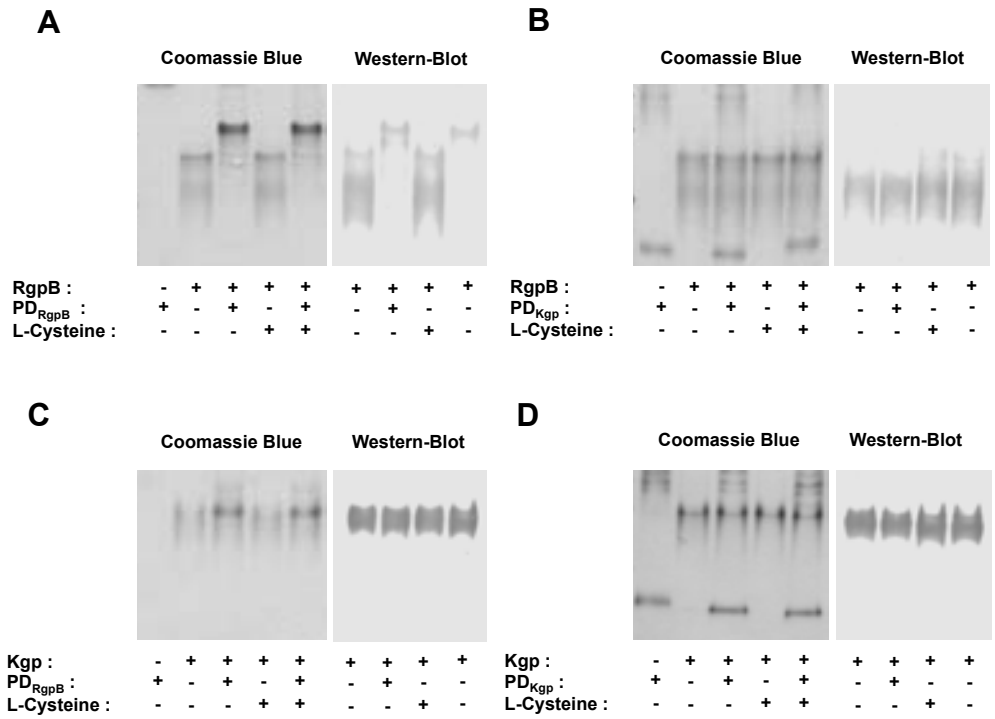
A
Coomassie Blue
Western-Blot
RgpB : - + + + + + + + +
PD$_{RgpB}$: + - + - + - + - -
L-Cysteine : - - - + + - - + -
B
Coomassie Blue
Western-Blot
RgpB : - + + + + + + + +
PD$_{Kgp}$: + - + - + - + - -
L-Cysteine : - - - + + - - + -
C
Coomassie Blue
Western-Blot
Kgp : - + + + + + + + +
PD$_{RgpB}$: + - + - + - + - -
L-Cysteine : - - - + + - - + -
D
Coomassie Blue
Western-Blot
Kgp : - + + + + + + + +
PD$_{Kgp}$: + - + - + - + - -
L-Cysteine : - - - + + - - + -

Figure 2

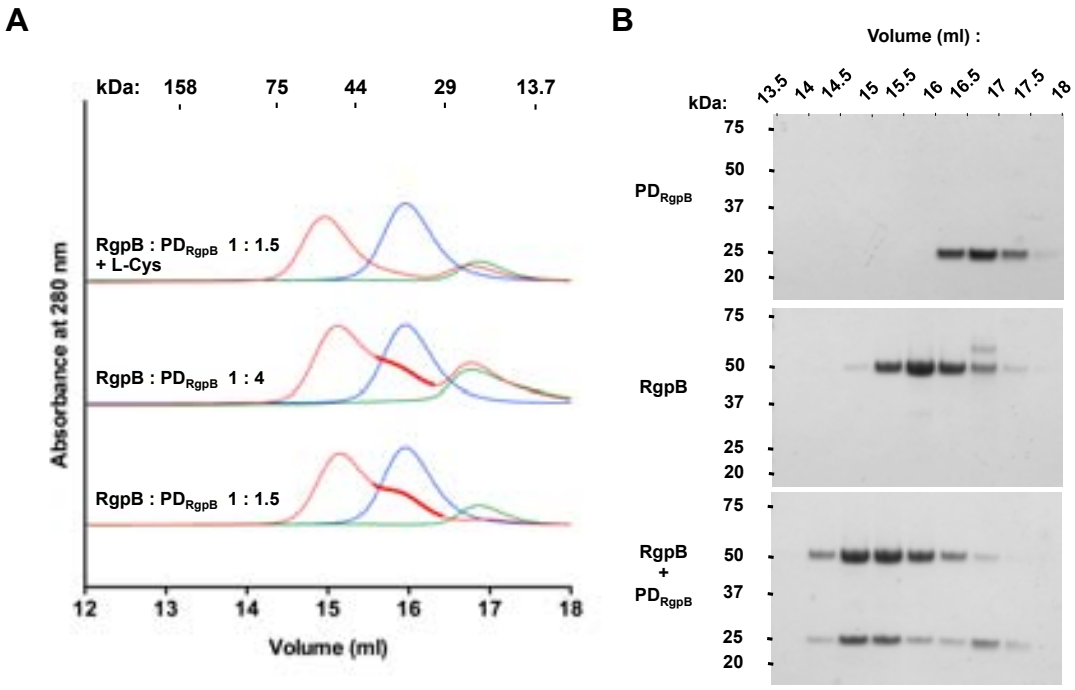
A
kDa: 158 75 44 29 13.7
RgpB : PD$_{RgpB}$ 1 : 1.5
+ L-Cys
RgpB : PD$_{RgpB}$ 1 : 4
RgpB : PD$_{RgpB}$ 1 : 1.5
Absorbance at 280 nm
12 13 14 15 16 17 18
Volume (ml)
B
Volume (ml) :
kDa:
13.5 14 14.5 15 15.5 16 16.5 17 17.5 18
PD$_{RgpB}$
RgpB
RgpB + PD$_{RgpB}$
75 50 37 25 20

Figure 3

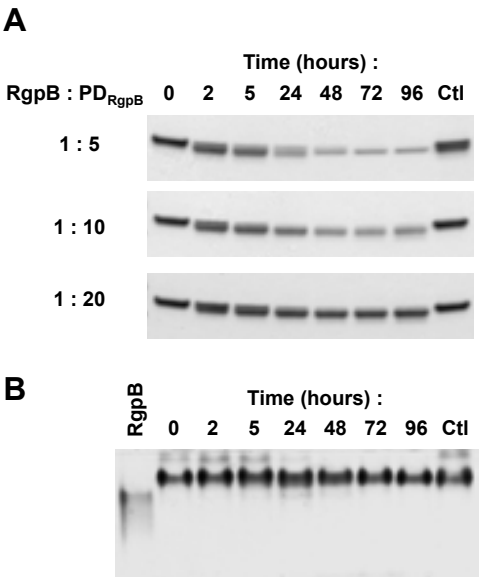
A
Time (hours) :
RgpB : PD$_{RgpB}$ 0 2 5 24 48 72 96 Ctl
1 : 5
1 : 10
1 : 20
B
RgpB
Time (hours) :
0 2 5 24 48 72 96 Ctl

Figure 4

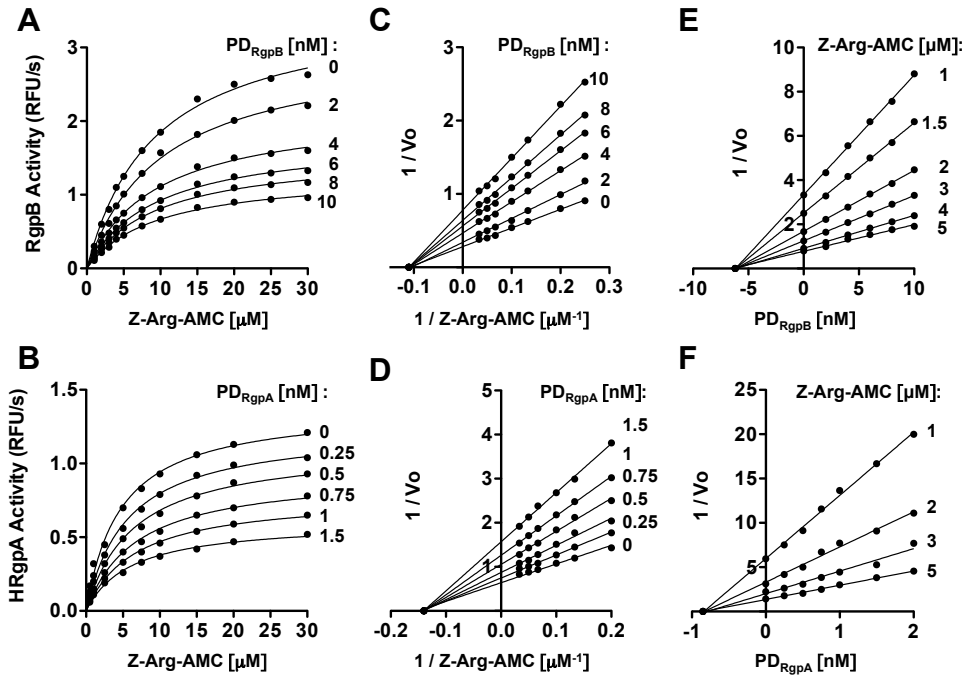
A
RgpB Activity (RFU/s)
PD$_{RgpB}$ [nM] :
0
2
4
6
8
10
Z-Arg-AMC [μM]
C
1 / Vo
PD$_{RgpB}$ [nM] :
10
8
6
4
2
0
1 / Z-Arg-AMC [μM^{-1}]
E
1 / Vo
Z-Arg-AMC [μM]:
1
1.5
2
3
4
5
PD$_{RgpB}$ [nM]
B
HRgpA Activity (RFU/s)
PD$_{RgpA}$ [nM] :
0
0.25
0.5
0.75
1
1.5
Z-Arg-AMC [μM]
D
1 / Vo
PD$_{RgpA}$ [nM]:
1.5
1
0.75
0.5
0.25
0
1 / Z-Arg-AMC [μM^{-1}]
F
1 / Vo
Z-Arg-AMC [μM]:
1
2
3
5
PD$_{RgpA}$ [nM]

Figure 5

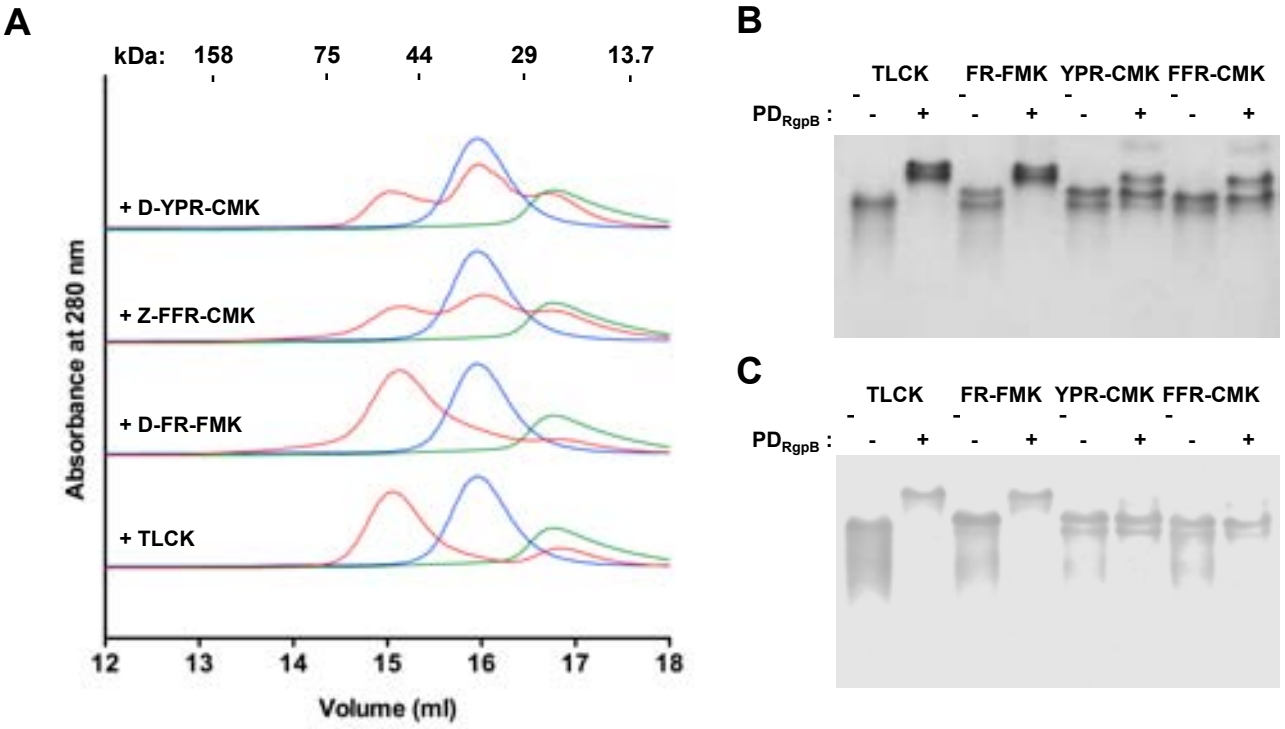

Figure 6

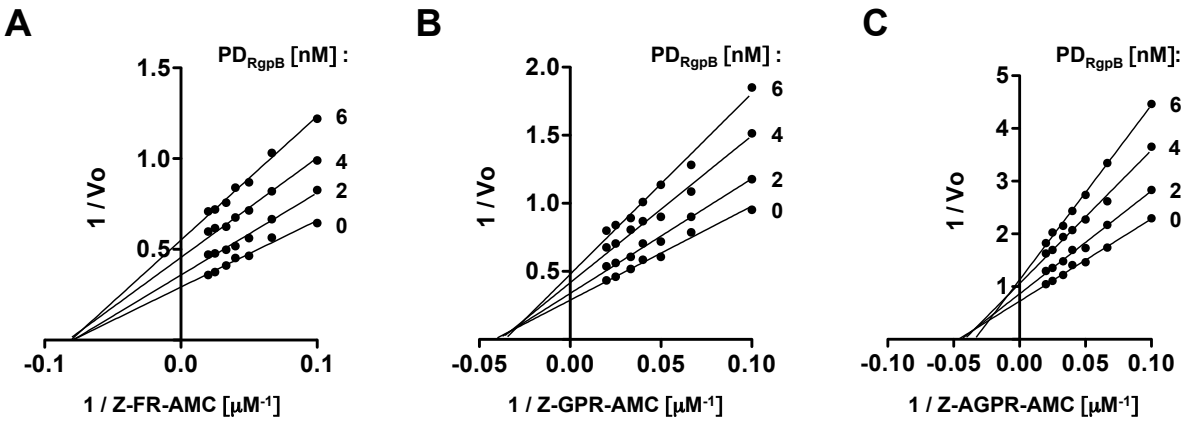

Figure 7

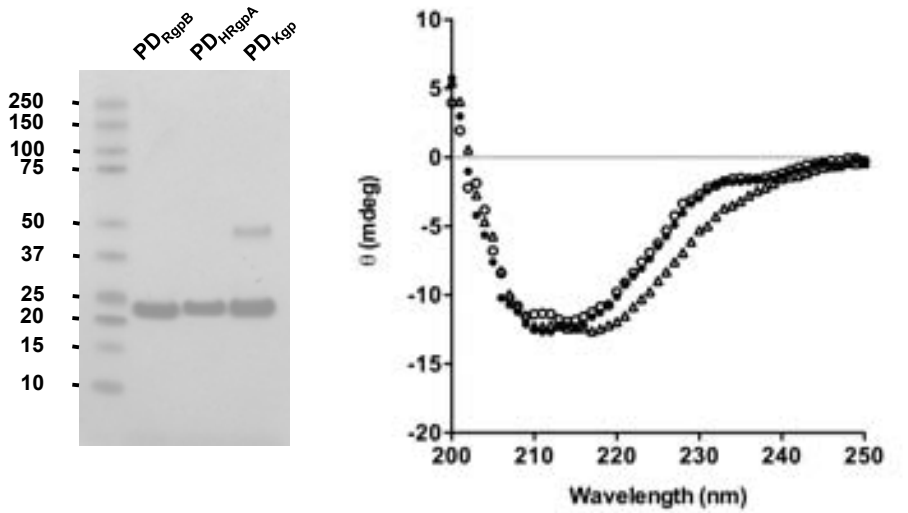

PD	Nbr of residues	MW (kDa)	pI	% Identity			% α-helixβ		% β-sheet	
				RgpB	RgpA	Kgp	Theoretical	CD spectra	Theoretical	CD spectra
PD_{RgpB}	205	22.8	8.06	-	75.7	20.7	5.4	6	39.5	47.6
PD_{RgpA}	203	22.9	9.47	75.7	-	19.8	5.9	7	37.9	46.5
PD_{Kgp}	204	22.3	5.95	20.7	19.8	-	7.8	7.1	40.7	46.5

Figure S1.

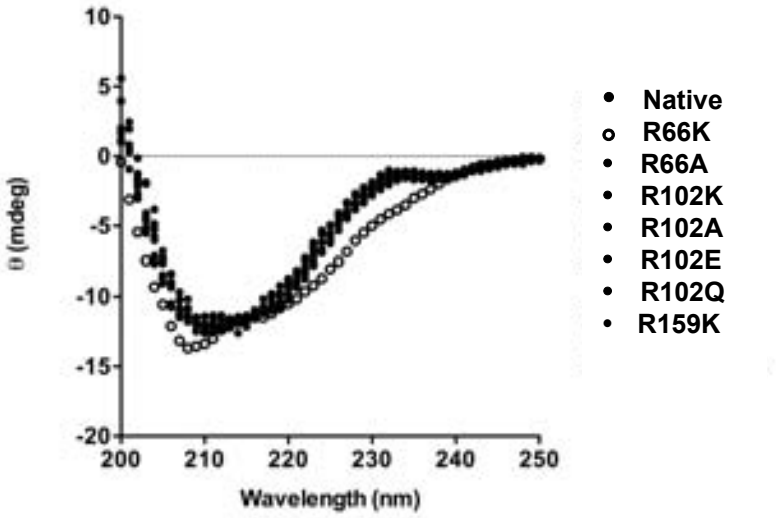

PD_{RgpB}	% α-helix	% β-sheet
Native	6	47.6
R66K	8	47
R66A	6	47.6
R102K	6	47.6
R102A	6	47.6
R102E	6	47.6
R102Q	6	47.6
R159K	6	47.6

Figure S2.

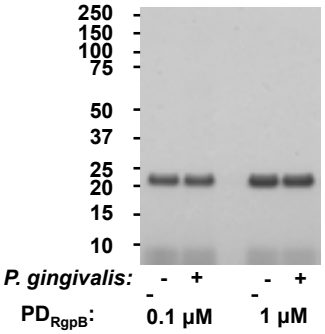

Figure S3

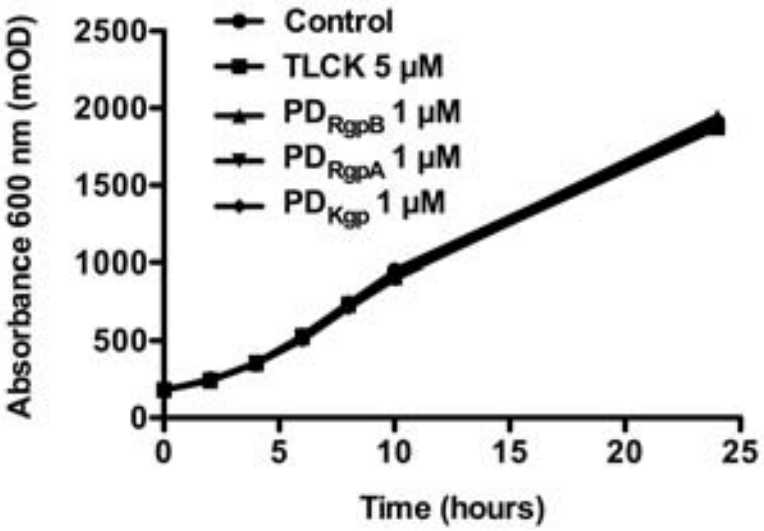
Absorbance 600 nm (mOD)
2500
2000
1500
1000
500
0
0
5
10
15
20
25
Time (hours)
Control
TLCK 5 µM
PD$_{RgpB}$ 1 µM
PD$_{RgpA}$ 1 µM
PD$_{Kgp}$ 1 µM

Figure S4